BT-1038.18

Skyhook Aerial Rescue System

Robert Fulton Co.

John H. Gilchrist

Oct 1967

XVIII. Skyhook Aerial Rescue System

John H. Gilchrist
Robert Fulton Company
Danbury, Connecticut

Abstract

A tethered balloon system developed as a land-to-air and sea-to-air system for inflight recovery of men and equipment is described. Balloon system and design parameters generated by operational requirements are included.

1. INTRODUCTION

Unlike most of the balloon systems about which we have heard in the context of this symposium, the balloons I wish to discuss are very small. They fly at a low altitude and support nothing but their own mass plus the mass of the tether line. In so doing, this tethered balloon system makes possible the saving of human life.

Fourteen years ago ONR asked Robert Fulton of Newtown, Connecticut, to develop a land-to-air and sea-to-air system for inflight recovery of men and equipment stranded in remote regions inaccessible to conventional modes of aerial retrieval. Several years later the feasibility of the Fulton Skyhook was demonstrated. Two years after that the first man-pickup took place. Since that time hundreds of day and night line pickups have been accomplished from jungle clearings, open water, the Arctic ice cap and the decks of ships. Today the ARRS alone has sixty HC 130H aircraft fully equipped with the Fulton Skyhook, capable of retrieving single pickup loads up to 500 lb within a 5000-mile radius.

2. OPERATION OF SKYHOOK

The rescue aircraft, a fixed-wing propeller plane exhibiting a yoke mounted on the nose for guiding the tether line into "home" position at intercept, is also provided with: (1) permanently installed electromechanical ("Skyanchor") and hydraulic (winch) equipment for effecting lock-on and load retrieval after intercept, and (2) drop kits containing rescue software which are parachuted to the survivor.

Let us run through the sequence of events of a Skyhook pickup, emphasizing those that precede the moment the survivor is actually airborne, since this is the phase in which the tethered balloon subsystem does its job.

Figure 1 presents a condensation of the initial sequence whereby the survivor receives his software and performs the ground-sea operation that will enable the rescue aircraft to retrieve him. Upon donning the harness-suit and removing the balloon and helium modules from their containers, he inflates the balloon to the indicated pressure and launches it to 500-ft altitude, the "anchor" end of the tether line secured to his harness straps. From this point the survivor simply waits for the aircraft to intercept the tether line, approximately 20 to 25 min from the time he receives the drop kits.

Figures 2 and 3 show in detail the survivor inflating the balloon, featuring the helium supply, inflation gear, and harness-suit. A fully inflated balloon, ready for launching, appears in Figure 4. Observe the "anchor" end of the tether line hooked into the shoulder straps behind the survivor, lower left. The balloon is a nonextensible, equal-pressure aerodynamic design, aspect ratio about 3:1, exhibiting static lifts ranging from 40 to 65 lb, according to whether the balloon is for a one-man (680 ft^3) or two-man (1200 ft^3) pickup.

With the balloon flying at altitude, the survivor sits back to wind, facing the direction from which the aircraft will make its approach for intercept (Figure 5). We will leave our friend for a moment while we consider the tactical operation facing the pilot overhead.

Figure 6 presents a panorama of øperations from a vantage point aloft. Observe in the center the man-tethered balloon system, the focus of both our attention and the pilot's. Notice too that the balloon serves three functions: (1) to hold aloft the tether line; (2) to present a visible target for the rescue aircraft; and (3) to enable the pilot to navigate a precise upwind approach for intercept by virtue of its directional properties.

Traveling at 125 knots, the aircraft flies its downward leg, losing altitude in such a way that upon circling into the final upwind leg the aircraft will intercept the tether line roughly 50 ft below the balloon.

This final maneuver calls for the exercise of judgment by the pilot in winds of sufficient intensity to cause the balloon-line system to "fall off" more than 20° from the vertical. He must adjust both his altitude and his angle of approach, in response to the severity of "fall-off," in order that upon intercept the initial portion of the survivor's trajectory will be as vertical as possible (see Figure 7).

Figure 8 features the configuration of the nose yoke on a twin-engine rescue aircraft, with a span of 25 ft and included angle of 105°. Less evident are the fending lines extending from wing tip to corresponding yoke, installed to prevent fouling of propellers in the event of a missed intercept. Figure 9 shows an HC-130H ARRS aircraft about to make an intercept; observe the relative positions of intercept point and balloon.

Let us now go back quickly to our survivor, who has been left waiting for his pickup (Figure 5). His line having been locked into the nose of the aircraft, he becomes instantaneously airborne as the line pulls vertically, the aircraft moving from left to right (Figure 10). The same moment of "lift-off" is recorded in the case of a dual pickup (Figure 11) in which the men are hooked together to minimize their relative motions as they ascend rapidly toward the aircraft (Figures 12 and 13). The shoulder straps are designed to compel the load to travel backwards once its trajectory develops an appreciable X-component of velocity.

In the final sequence of photographs (Figures 14, 15, and 16), the men are reeled into the aircraft by means of a hydraulic winch in the rear bay. The view offered by Figure 16 makes it possible to discuss the changing relationship of tether line to aircraft, from moment of lock-on at the nose until this same line is transferred to the winch in the rear. As the load reaches the level portion of its trajectory, the tether line under the aircraft also rises to the point where a crewman may engage it as the line passes directly under the rear bay. How the line appears from the bay, after engagement by the winch, is shown in Figure 17.

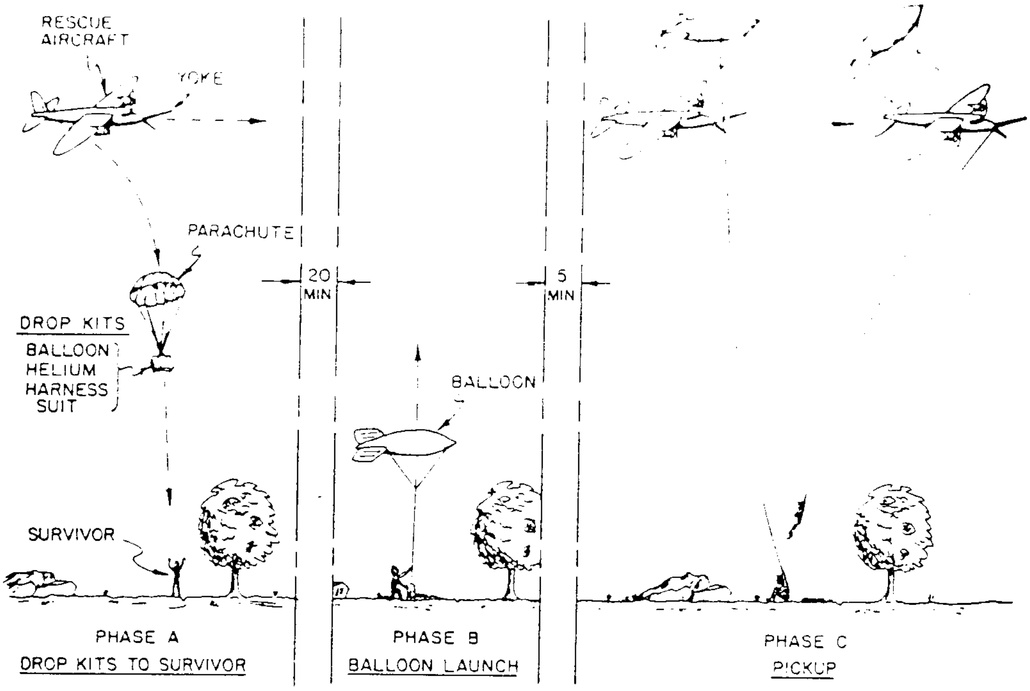

Figure 1. Fulton Skyhook Sequence of Events

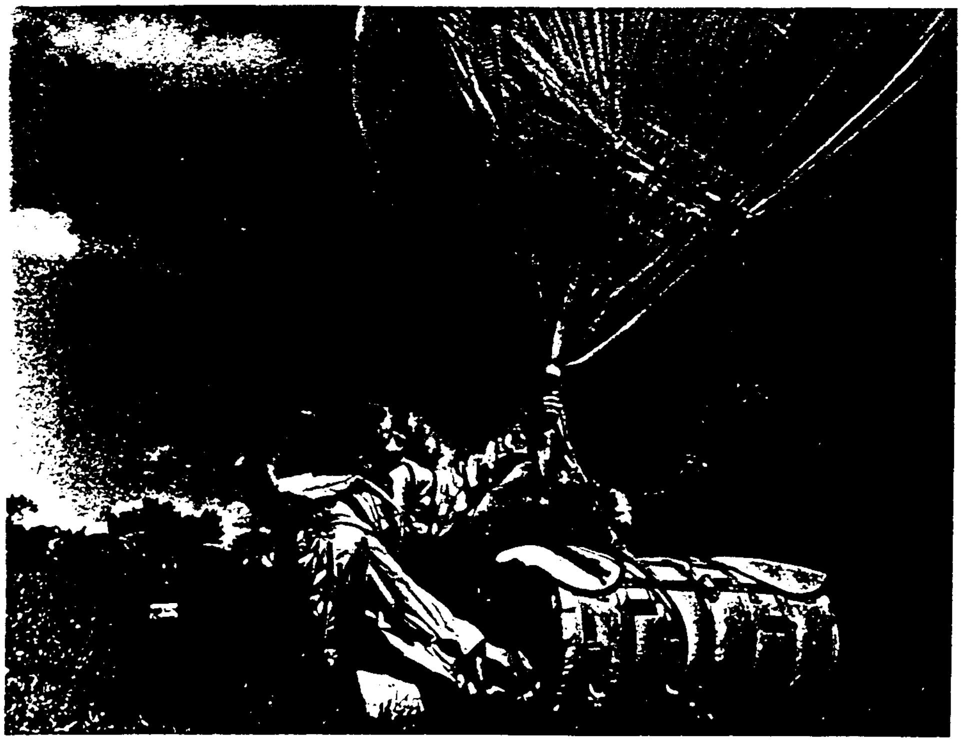

Figure 2. Balloon Inflation Showing Helium Supply, Inflation Gear, and Harness-suit

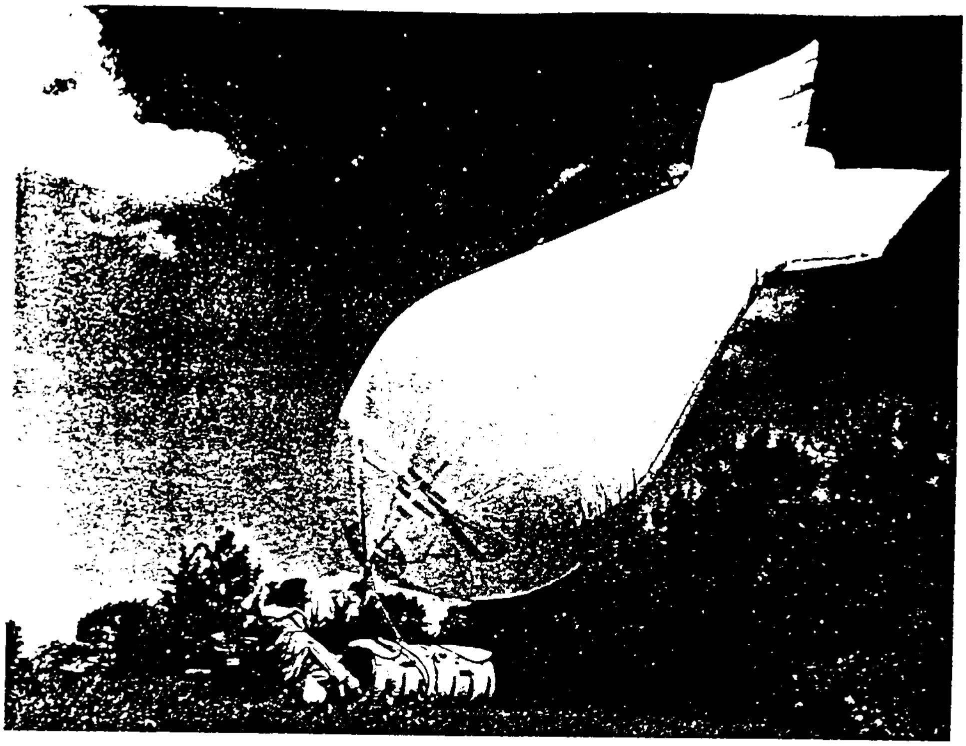

Figure 3. Balloon Inflated

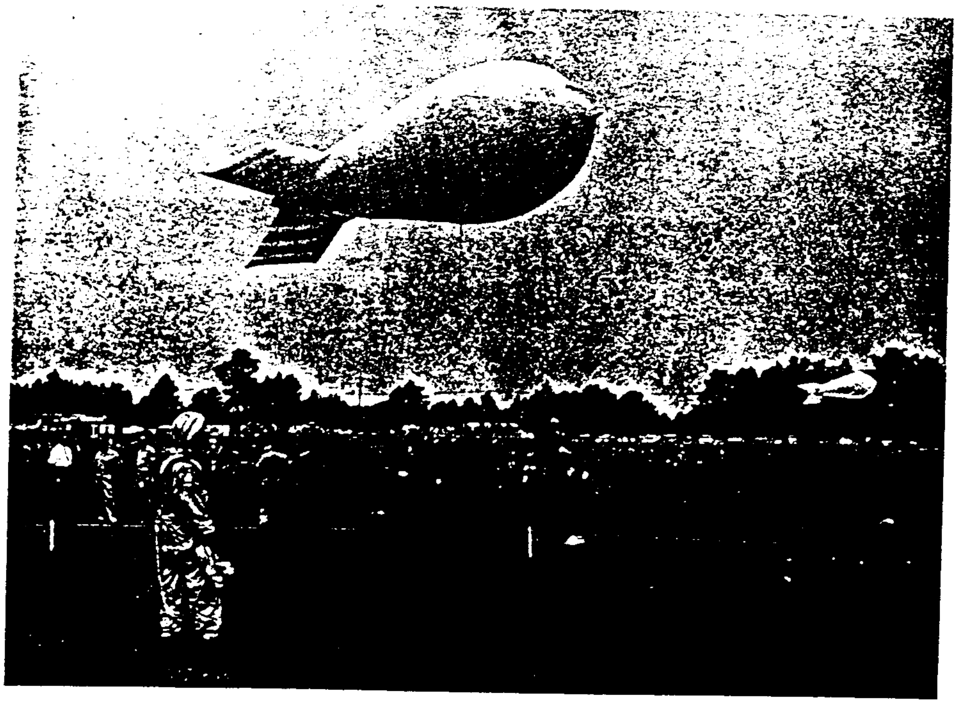

Figure 4. Fully Inflated Balloon Ready for [illegible]

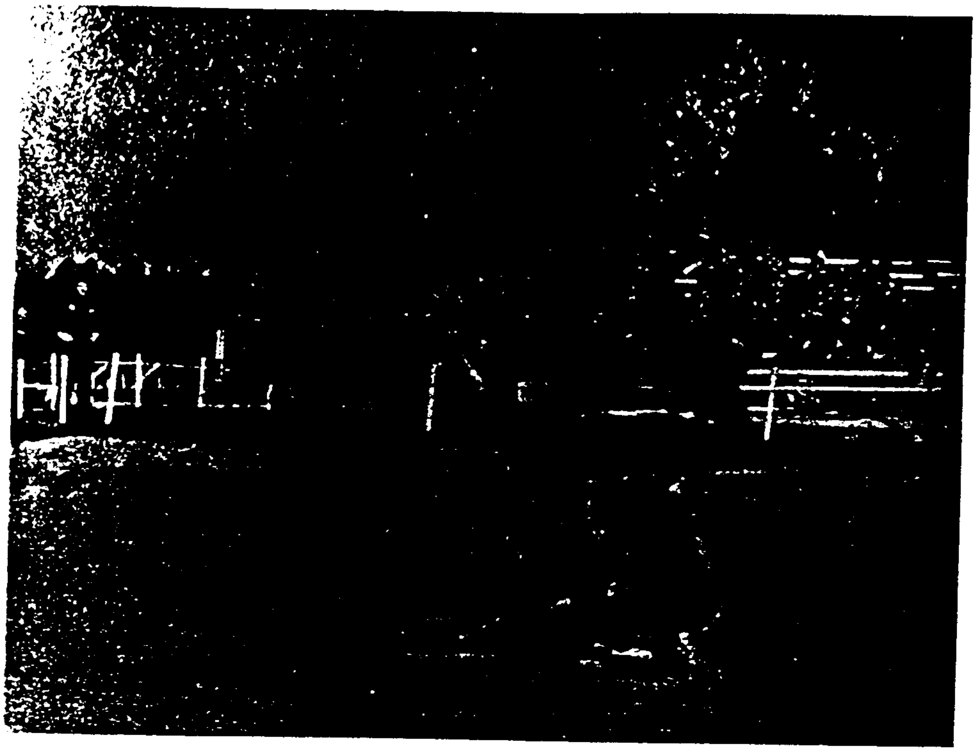

Figure 5. Survivor Ready for Pickup

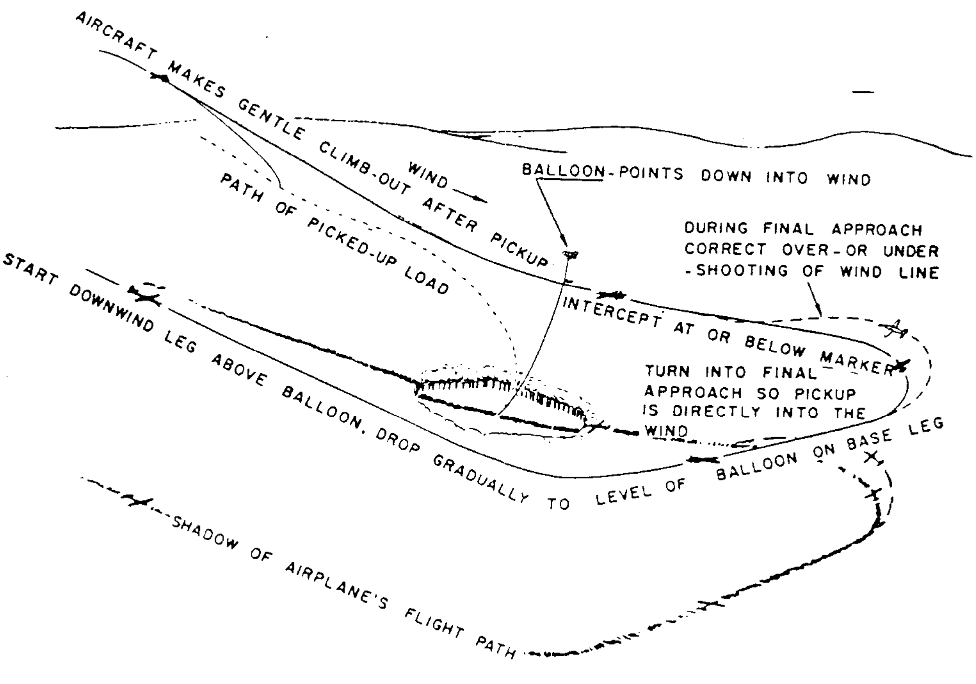

Figure 6. Fulton Skyhook Pilot Technique

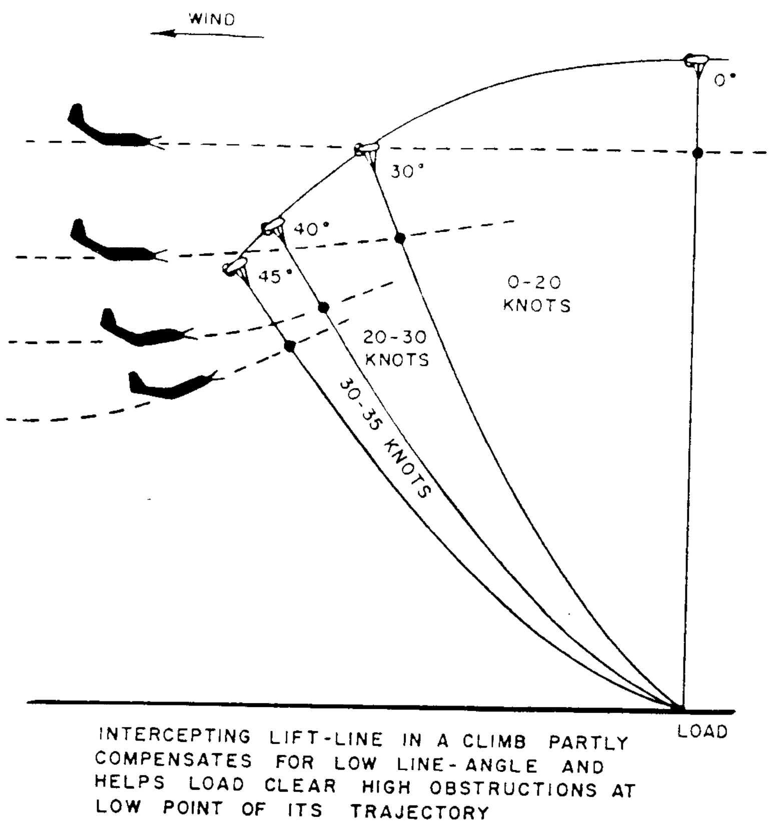

Figure 7. Line and Intercept Angles Versus Wind

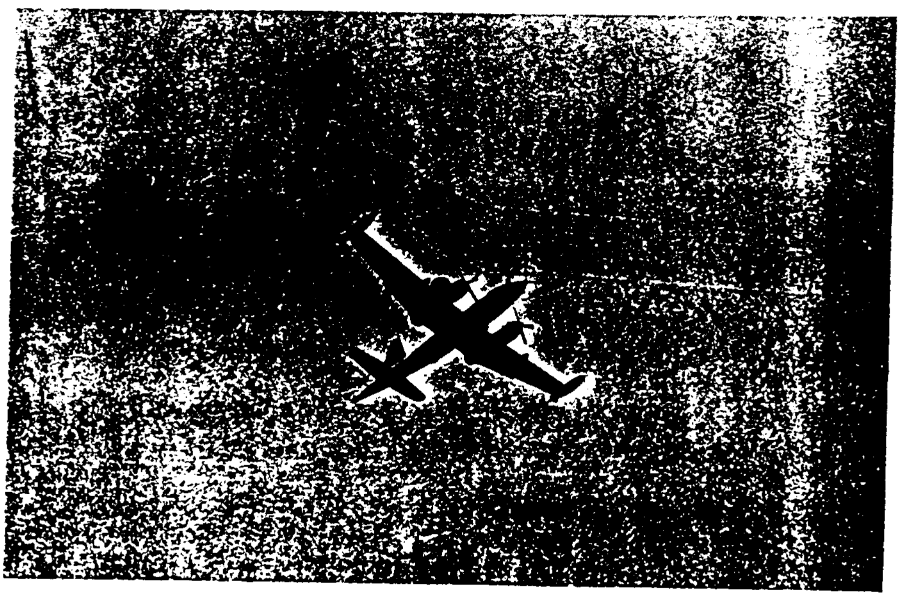

Figure 8. Nose Yoke Configuration on a Twin-Engine Rescue Aircraft

Figure 9. HC-130H ATRS Aircraft About to Make an Intercept

[illegible] 10. [illegible]

Figure 11. Dual Pickup

Figure 12. Men Ascending Toward Aircraft

Figure 13. Men Ascending Toward Aircraft

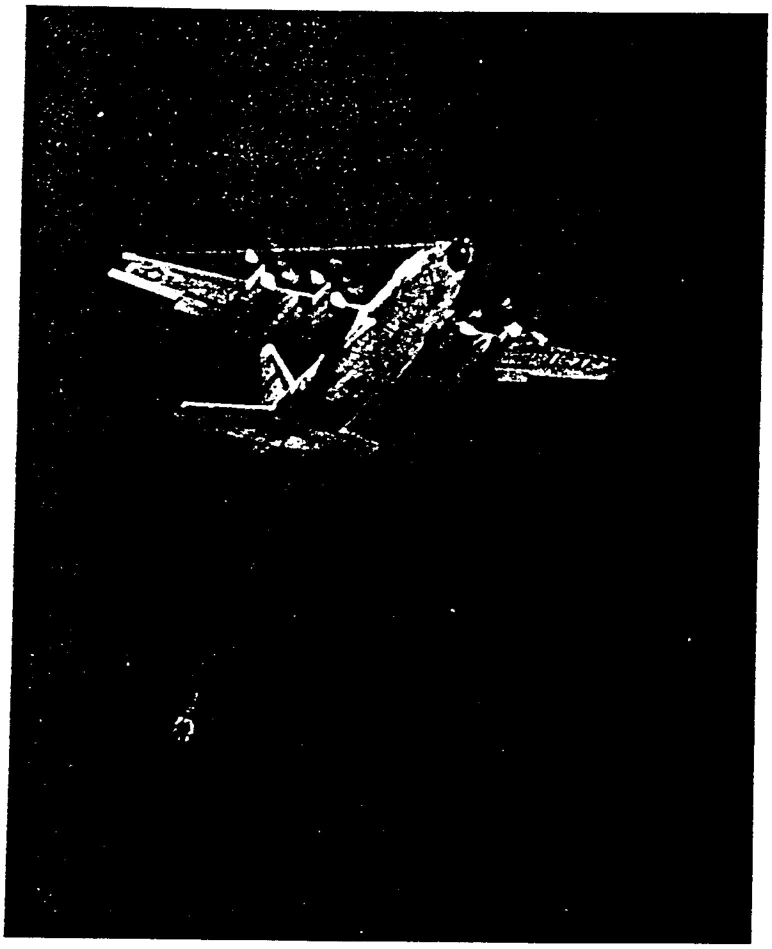

Figure 14. Men Being Reeled into Aircraft

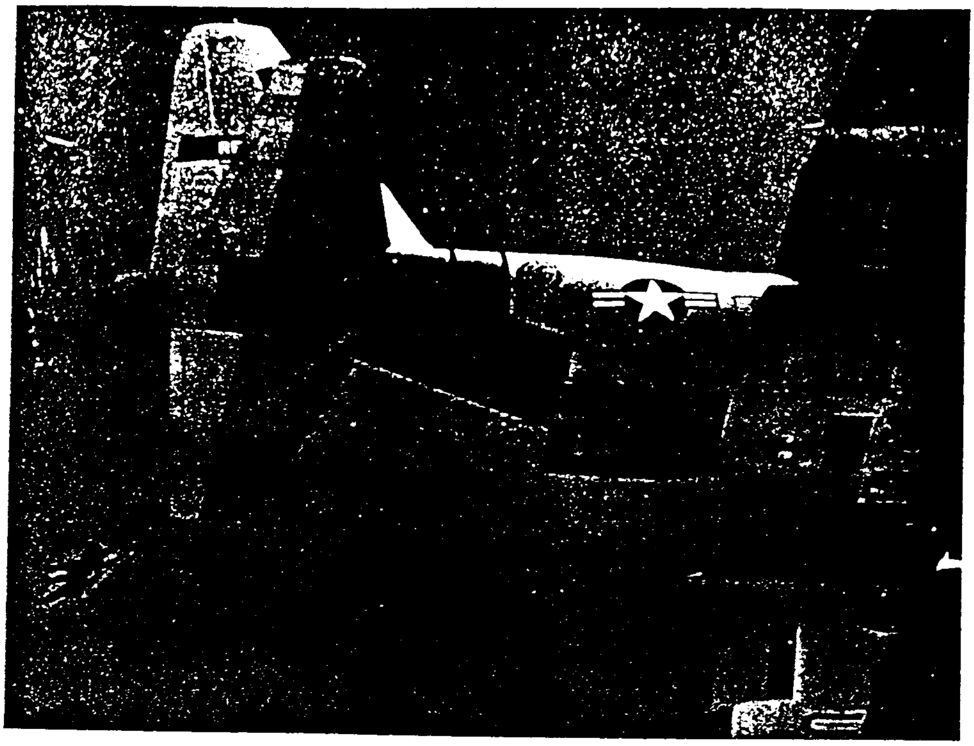

Figure 15. Men Approaching Aircraft

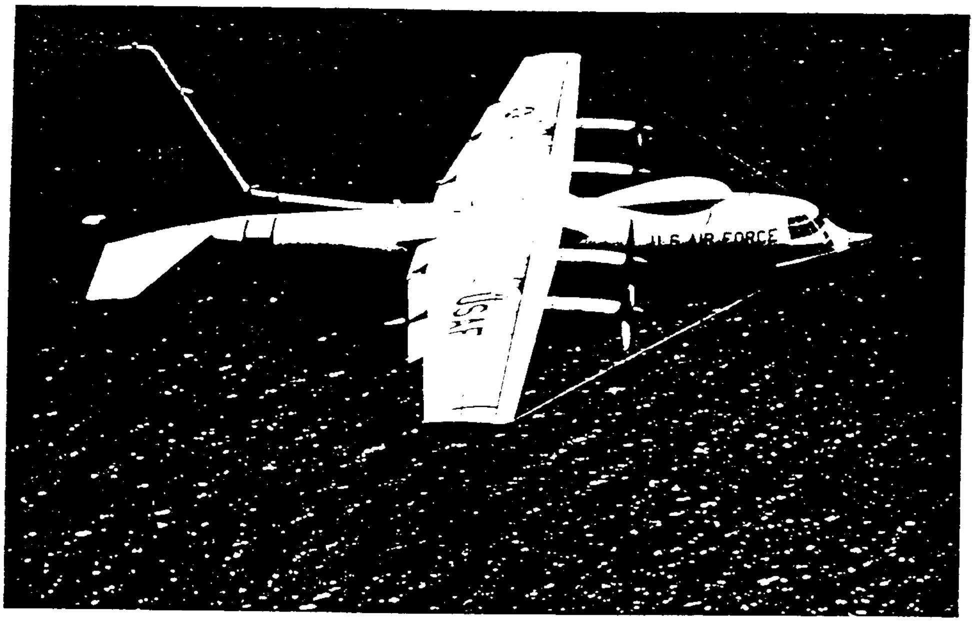

Figure 16. Full View of Men Approaching Aircraft

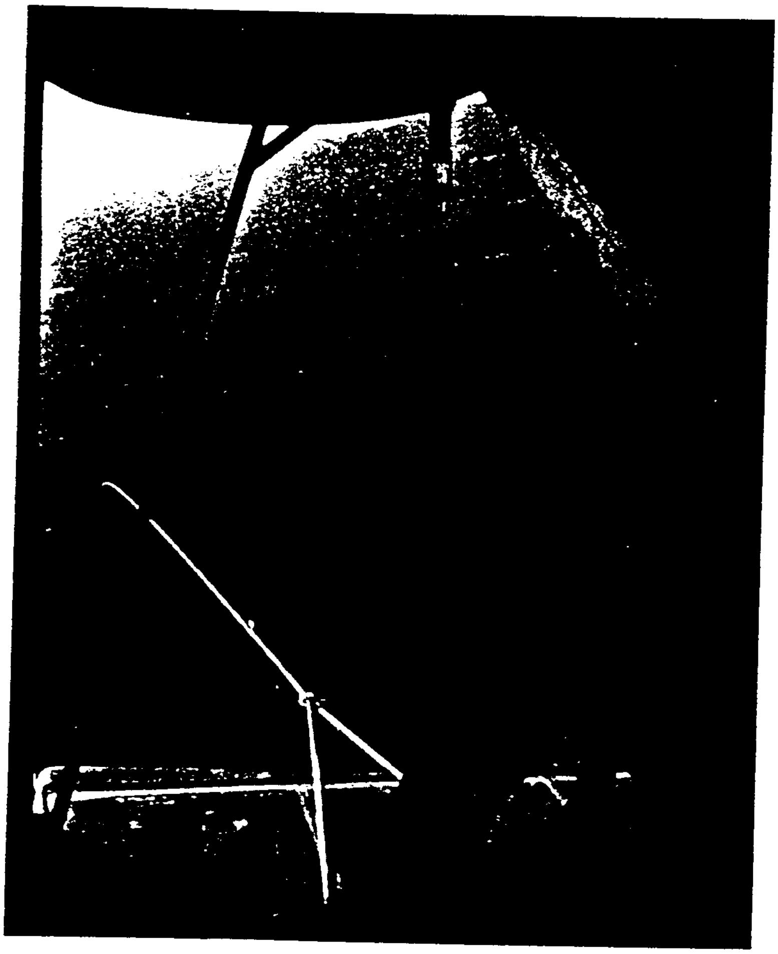

Figure 17. View of Line as Seen from Aircraft Bay

Appendix A

Mechanics of Load Trajectory

1. Cycloidal Theory

In Figure A1, if the ordinate of 0 horizontal distance is considered the Y-axis, that of 0 vertical distance the X-axis, and their point of intersection the origin "0," let us superimpose a linear time scale along the X-axis, negative to the left of the origin and positive to the right.

If time "0" coincides with the moment the aircraft intercepts the tether line, negative time corresponds with the existence of a simple, static man-tethered balloon system, positive time with the existence of a dynamic, free man-aircraft system experiencing translatory and rotational motion. More specifically, at "0" time interception of the tether line instantaneously converts the man-tethered balloon system into the kinematics of a generating "cycloid" whose "cycloidal" path is described by the man-load as the point on a circle rolling along the X-axis with center determined by the flight path of the aircraft, and generating radius defined by the tether line uniting man and aircraft.

The term "cycloid" is placed in quotation marks because there is no *a priori* reasoning to indicate that the actual trajectory *is* cycloidal, or even trochoidal, simply the existence of forces so related geometrically as to suggest the cycloid is a highly plausible result of their interaction *for the initial part (180 ft) of the trajectory only*; beyond this point, forces like gravity and wind resistance probably supervene to account for the rapid departure of the trajectory from the equivalent cycloid

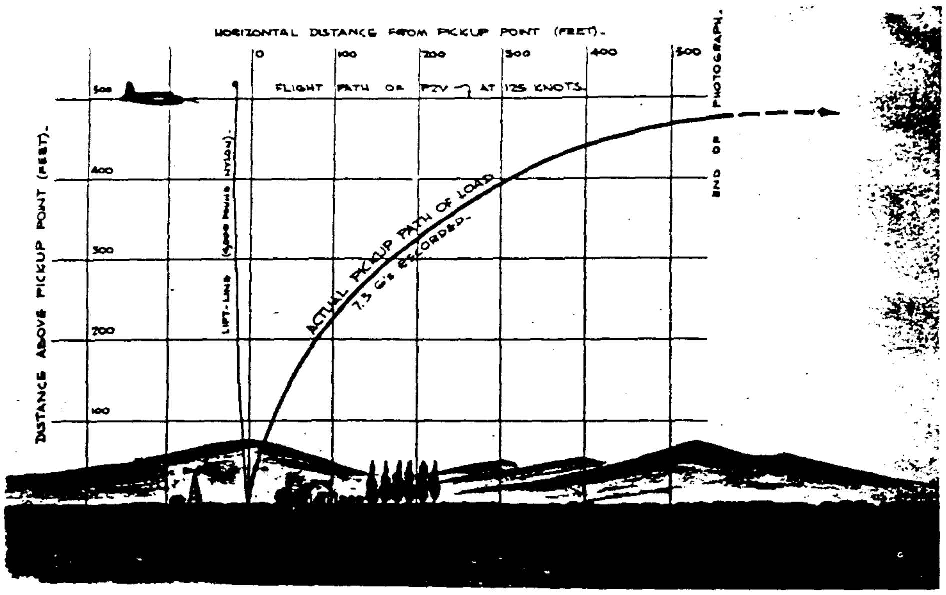

Figure A1. Skyhook Trajectory

on which it began. Thus one may think of the initial portion of the trajectory as reflecting the instantaneous kinematics (that is, at pickup or lift-off) of a cycloid that presently (2 sec later) merges into a curve increasingly responsive to the dynamics of a mass particle obeying the three forces whose equilibration ultimately establishes the steady-state condition of motion – gravity, wind drag, and tether line tension. Except for the fact that line elasticity will undoubtedly introduce a time delay in the initial lift-off velocity and acceleration, there is evidence that the initial trajectory both kinematically and graphically approximates the equivalent cycloid, with these parametric equations of motion:

Load velocity:

$$\frac{ds}{dt} = \omega \sqrt{\rho a \sin \tfrac{1}{2} \phi} \tag{A1}$$

Tangential acceleration:

$$\frac{d^2s}{dt^2} = \omega^2 a \cos \tfrac{1}{2} \phi \tag{A2}$$

Normal acceleration:

$$\frac{1}{\rho}\left(\frac{ds}{dt}\right)^2 = \omega^2 a \sin \tfrac{1}{2}\phi \tag{A3}$$

where

ϕ = generating angle at time t

$\omega = \frac{d\phi}{dt}$ = angular velocity of generating circle

ρ = radius of curvature of cycloid at time t

a = aircraft altitude (tether length)

Support for the cycloidal theory is found in tracings from photographs showing the changing relationship of load trajectory to intercept altitudes. In Figure A2 we see as aircraft altitude diminishes, the corresponding peak is relatively higher, which follows from Eq. (A2) in which acceleration in the direction of motion is a function of ω^2, but of a (intercept altitude) to the first power only. That the absolute peaks are progressively lower as intercept altitude diminishes follows from Eq. (A3) where $\sin \frac{1}{2}\phi$ predominates over $\cos \frac{1}{2}\phi$ sooner at time t, the smaller generating circle.

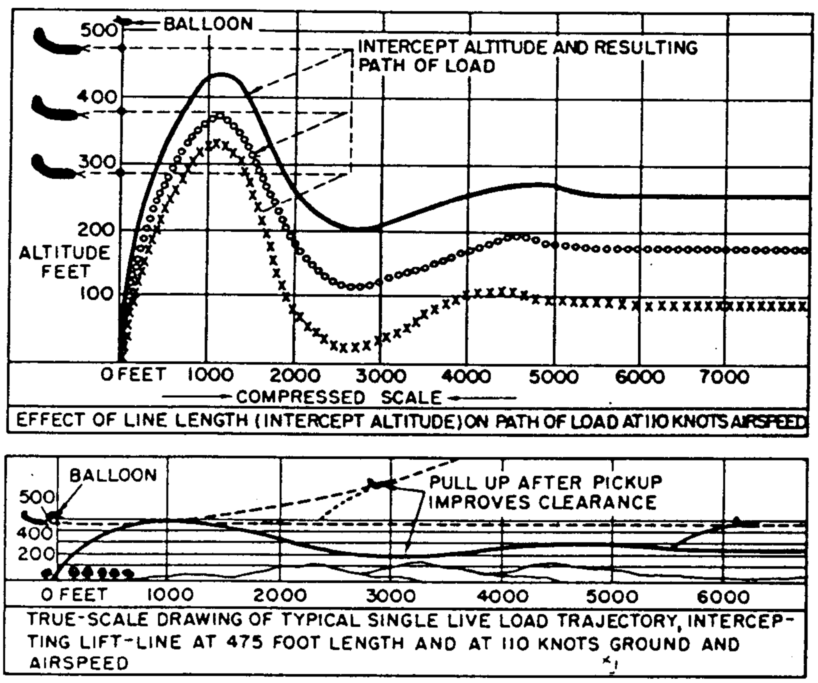

Figure A2. Effect of Intercept Altitude on Load Trajectory

2. Balloon Drag – Correlation Study

I should like to conclude with a note about drag on which some of you may be able to shed light.

We have attempted to correlate field measurements of balloon drag with drag values predicted by empirical friction formulations developed by German investigators in the past. The graph (Davidson, 1936) in Figure A3 exhibits the classical relationship of the coefficient of frictional resistance (C_f, or drag) to Reynolds number for any totally submerged body in the Reynolds number range relevant to our balloon work.* In physical terms, since a body submerged in a moving fluid experiences resistance (drag) essentially frictional in nature, the relationship shown is actually a plot of the trend of the ratio of normal to shearing stresses in fluid particles within the boundary layer, as a function of Reynolds number.

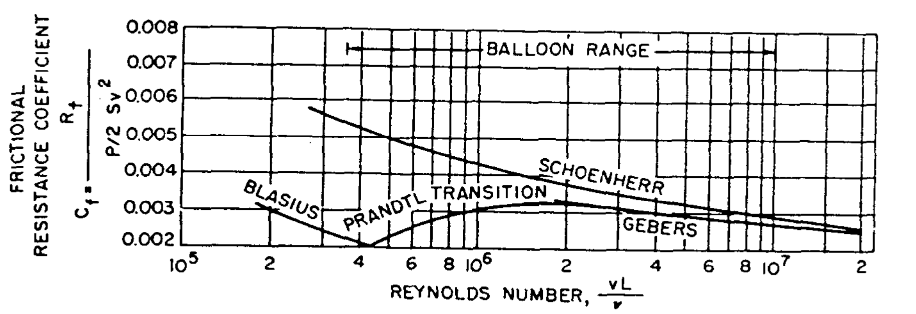

SEMILOG CHART OF C_f VS REYNOLDS NUMBER - EMPIRICAL FRICTION FORMULATIONS

$R_e = 1.08\ VL \times 10^4$

$R_f = 0.107\ C_f\ SV^2$

BALLOON		WIND SPEED (v) KNOTS	R_e $\times 10^6$	C_f			R_f LBS
LENGTH (L) FT	AREA (S) FT^2			B	P	G	
16	190	2	.34	.0022			1.8
		30	5.1			.0030	5.4
19	250	2	.42	.0020			2.2
		30	6.3			.0028	67
26	480	2	.56		.0024		5.0
		30	8.5			.0026	120
31	680	2	.65		.0026		7.6
		30	9.7			.0026	170

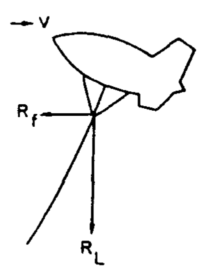

Figure A3. Balloon Drag (R_f) and Classical Fluid Friction Data

*Of particular interest is the fact that this range encompasses the whole of the "transition" region, between laminar and turbulent flow.

The table of Figure A3 indicates the derivation of "classical" predicted drag (R_f) values applied to our balloons, using the expressions appearing to the left of the table. These values of R_f are two to threefold R_f drag values observed in the field, obtained by solving the right triangle defined by measured tether line tension and observed angle of tether line with the vertical where it meets the shroud lines.

Two possible explanations present themselves:

1. Is it credible that measured field values of R_f are low because they actually represent "residual" drag, that is, absolute drag* minus a forward-directed drive such as exists in yacht sails going to windward (Davidson, 1936)? Positive evidence for this "drive-force" in balloons appears in their capacity to fly at the zenith, or slightly upwind of it, in light winds of 5 to 8 knots.

2. Is boundary layer flow actually laminar in the R_e balloon range, despite theory and empirical evidence suggesting it should be transitional-to-turbulent?

In any case, these very tentative answers point to a need for exhaustive field and wind-tunnel studies to illuminate this area of balloon aerodynamics.

References

Davidson, K.S.M. (1936) Some experimental studies of the sailing yacht, Proc. Soc. Nav. Architects and Marine Engrs 44:301.

Op. cit., 294-295.

---

*Drag plus induced drag (due to a finite angle of attack)